Catalysis Letters 23 (1994) 321–337

Preparation and characterization of three pure magnesium vanadate phases as catalysts for selective oxidation of propane to propene

Xingtao Gao [a], P. Ruiz [b], Qin Xin [a], Xiexian Guo [a] and B. Delmon [b]

[a] *State Key Laboratory of Catalysis, Dalian Institute of Chemical Physics,*
Chinese Academy of Sciences, Dalian 116023, PR China
[b] *Université Catholique de Louvain, Unité de Catalyse et Chimie des Matériaux Divisés,*
Place Croix du Sud 2, boite 17, 1348 Louvain-la-Neuve, Belgium

Received 11 June 1993; accepted 22 September 1993

Three magnesium vanadate phases, i.e., MgV_2O_6 (metavanadate), α-$Mg_2V_2O_7$ (pyrovanadate) and $Mg_3V_2O_8$ (orthovanadate), have been successfully prepared with high purity by the citrate method at a relatively low temperature (550°C). FT-IR, LRS, XRD and SEM techniques have been used to characterize these vanadate phases. The effect of calcination temperature has also been investigated. It was found that the particle size and morphology of the MgV_2O_6 phase, which is a function of calcination temperature, appear to have a strong effect on the infrared spectra. Furthermore, the catalytic properties of the three phases were examined in the oxidative dehydrogenation of propane. The propene selectivity follows the order: α-$Mg_2V_2O_7 > Mg_3V_2O_8 > MgV_2O_6$, which is consistent with their redox properties. This fact suggests that there is some correlation between the catalytic and redox properties of these magnesium vanadate phases.

Keywords: Citrate method; magnesium vanadates; redox property; selective oxidation of propane to propene

1. Introduction

The transformation of alkanes into useful intermediates is presently the object of intense investigation in the field of catalysis. The V–Mg–O catalysts have been proposed to be active and relatively selective in the oxidative dehydrogenation of propane [1,2]. Three Mg vanadate phases can be formed in the V–Mg–O catalysts as a function of vanadium concentration and calcination temperature [3]. However, contradictory results have been obtained in the previous studies on catalysts concerning the active phase responsible for the formation of alkene. Kung and coworkers [1,2,4] attributed the active phase to Mg orthovanadate ($Mg_3V_2O_8$). But

Volta and co-workers [3] suggested that Mg pyrovanadate (α-$Mg_2V_2O_7$) was the active phase, and orthovanadate ($Mg_3V_2O_8$) was responsible for total oxidation.

When the activity and selectivity of a catalyst are considered, some factors must be taken into account, in particular, the preparation method and contamination by residual elements. To illustrate this point, a recent paper published by Kung [5] deals with the effect of potassium on the reactivity of V–Mg–O catalysts. The assignments of the active phase for V–Mg–O catalysts by the two research groups mentioned above were mostly based on the study of the three Mg vanadate phases. However, the calcination conditions they used to prepare these pure vanadates were very different from that of V–Mg–O working catalysts. The fact that they used high calcination temperatures (at least 650°C) and very long calcination times is due to their preparation method by solid–solid reactions.

Great differences in the infrared and Raman spectra of Mg vanadate phases also exist in literature [3,4,6,7]. This is partially due to the phase impurities originating from the traditional preparation method. Indeed, the reaction between magnesium oxide and vanadium oxide does not easily go to completion, as used with solid–solid reactions. The calcination temperatures, which control the particle sizes and morphologies of the microcrystals, will be shown in the present paper to be an important factor in determining the infrared spectra of MgV_2O_6 phase.

In this work, we used the citrate method to prepare the three pure Mg vanadate phases, i.e., MgV_2O_6 (metavanadate), α-$Mg_2V_2O_7$ (pyrovanadate) and $Mg_3V_2O_8$ (orthovanadate) under exactly the same conditions. This method provides the following advantages: (a) the expected oxide compounds can be obtained from very homogeneous citrate precursors; (b) lower calcination temperature can be used (550°C); (c) higher surface area for each Mg vanadate phase can be realized; (d) contamination from other residual elements can be minimized, as evidenced by XPS measurement.

The present work will focus on the detailed characterization of three Mg vanadate phases by XRD, IR, LRS and SEM techniques. The influence of calcination temperature on the physico-chemical properties of Mg vanadate phases was investigated. The relationship between the redox properties of the pure Mg vanadate phases and their catalytic properties in the oxidative dehydrogenation of propane was also suggested.

2. Experimental

2.1. CATALYST PREPARATION

The three Mg vanadate phases with Mg/V atomic ratios equal to 1/2, 1/1 and 3/2 were prepared by the citrate method [8]. The starting materials used were $Mg(NO_3)_2 \cdot 6H_2O$ and NH_4VO_3 (p.a.; ucb). The main steps of the citrate method are as follows:

(i) Preparation of a transparent solution of magnesium nitrate and ammonium metavanadate in such a concentration that the atomic ratio Mg/V in solution is equal to that in the resulting catalyst.

(ii) Addition of a small amount of 65% HNO_3 (0.1/250 ml) in order to avoid precipitation.

(iii) Addition of citric acid in such a manner that the molar number of equivalent anions (3 ions per molecule of citric acid) is equal to that of cations (Mg^{2+} and V^{5+}).

(iv) Evaporation of the obtained solution in a Rotavapor, initially at 40°C under reduced pressure until the solution becomes viscous, and then at ca. 90°C until a solid is obtained (amorphous organic precursor).

(v) Decomposition of the obtained solid at 380°C for 18 h and finally calcination at 550°C for 6 h. In order to investigate the influence of calcination temperature on the physico-chemical properties of the Mg vanadate phases, samples were further calcined at 650°C, 700°C or 750°C for another 6 h.

2.2. CATALYST CHARACTERIZATION

The BET sample areas were determined by krypton ($S_{BET} < 20$ m^2/g) or nitrogen adsorption ($S_{BET} > 20$ m^2/g) in an automatic apparatus ASAP 2000 constructed by Micromeritics.

X-ray diffraction was performed on a Siemens Diffrac-500 equipped with Cu Kα radiation. A JCPDS-ICDD (1990-1991) standard spectra software was used to determine the phases.

Scanning electron microscopy was performed on an AMRAY KY-1000B microscope.

Infrared spectra were recorded between 1200 and 350 cm^{-1} with a Bruker IFS 88B. The sample was mixed with KBr (2/300 by weight) and pressed into a thin wafer.

Raman spectra were collected with a Jobin Ivon Ramanor U-1000 double monochromatic spectrometer. The samples were pressed into self-supporting 15 mm diameter wafers and mounted in a rotating plate. The spectra were collected using as exciting radiation the 514.5 nm line of a Spectra-Physics series 2000 Ar ion laser. The laser power used was 200 mW (measured at the source).

DTA measurements were performed on a Perkin-Elmer DTA 1700 over the temperature range 40–900°C. Sample (30–40 mg) was contained in a platinum crucible set in a ceramic block and the heating rate was 10°C/min. All curves were obtained in dry air with a flow rate of 40 ml/min.

The thermogravimetrical study was conducted in a microbalance coupled to a vacuum system. Pretreatment, reduction and reoxidation were realized at 460°C. The gas flow rate was kept at 50 ml/min. Since Mg^{2+} ions are not reduced in the present conditions, the weight loss is calibrated to the reduction degree of vanadium ions in each sample (0% referred to V^{5+}, 100% of V^0). The procedure for this experiment was as follows: The sample was first pretreated at 460°C in vacuum for about half an hour until a steady weight was reached. Then nitrogen was introduced into the system. After the microbalance was stable, the gas system was switched to hydrogen. When the reduction finished, the system was evacuated and washed with nitrogen. After that, the reduced sample was reoxidized by switching to oxygen. The weight loss and weight gain were measured by a recorder which was connected to the microbalance.

2.3. CATALYTIC TEST

The catalytic test was performed in a flow system. The sample with particle fractions between 500 and 800 μm was placed on a fixed bed (inner diameter 15 mm) in a U-type quartz microreactor. Under standard conditions, the feed was 4 vol% propane (UCAR, IP), 8% oxygen and the balance He. The total flow rate was 50 ml/min. The experiments of selectivity as a function of conversion were performed by changing the catalyst weight used for reaction. The empty reactor showed no activity. No noticeable deactivation was observed during the test.

The reaction products were analyzed by on-line gas chromatography, using a Shimadzu C-R6A equipment. Helium was the carrier gas. Two columns were used in parallel. A VZ-7 (60/80 mesh, Alltech Associates, Inc.) column was used at 40°C to separate the hydrocarbons and CO_2. A molecular sieve 5A column was used to separate O_2 and CO. The conversion of propane is defined as the percentage of propane feed which has reacted. The propene selectivity is defined as the percentage of propane which reacts to propene.

3. Results

3.1. X-RAY DIFFRACTION

Fig. 1 illustrates the XRD spectra of the three Mg vanadate phases after calcination at 550°C. They are in good agreement with the standard spectra [9–11]. Identical spectra were obtained after calcination at 650°C. Very little phase impurities in α-$Mg_2V_2O_7$ and $Mg_3V_2O_8$ are detected. These small impurities are not easy to define, because the position of the reflection lines cannot fit well with the standard spectra of other magnesium vanadates or other possible phases. Higher calcination temperature appears to enhance the crystallinity, as indicated by the increasing intensity and sharpening of the XRD reflections of phases.

The unit cell parameters calculated from *d* values of the XRD spectra of three Mg vanadate phases are presented in table 1, in good agreement with the standard values. The color and surface area are also mentioned in table 1. It is noted that the surface area of each Mg vanadate phases decreases considerably as the calcina-

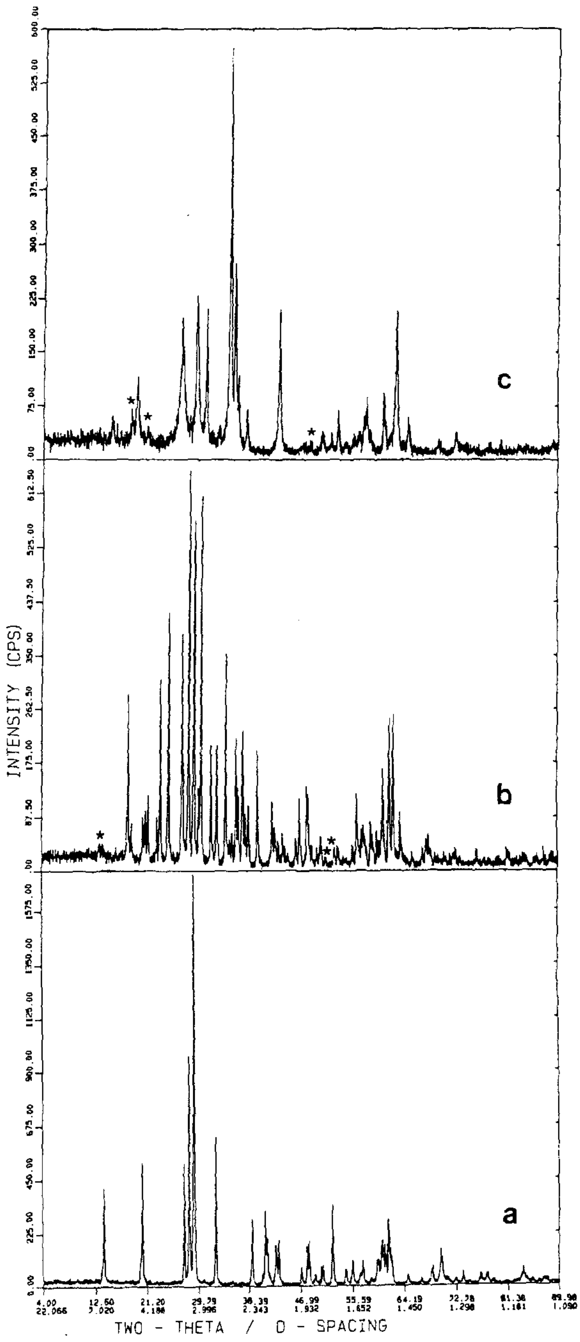

Fig. 1. X-ray diagram of (a) MgV_2O_6 550°C; (b) α-$Mg_2V_2O_7$ 550°C; (c) $Mg_3V_2O_8$ 550°C. (*) impurities.

Table 1
Comparison of three magnesium vanadate phases

	Phase		
	MgV_2O_6	α-$Mg_2V_2O_7$	$Mg_3V_2O_8$
colour	yellow	milk-white	white
surface area	2.7 (550°C) 0.7 (650°C)	8.3 (550°C) 4.5 (650°C)	22.8 (550°C) 9.7 (650°C)
unit cell parameters [a]	$a = 9.279$ $b = 3.502$ $c = 6.731$ $V = 203.12$ $\beta = 111.77°$	$a = 6.605$ $b = 8.415$ $c = 9.487$ $V = 518.27$ $\beta = 100.41°$	$a = 6.062$ $b = 11.439$ $c = 8.314$ $V = 576.52$
unit cell parameters [b]	$a = 9.293$ $b = 3.490$ $c = 6.736$ $V = 202.99$ $\beta = 111.73°$	$a = 6.612$ $b = 8.423$ $c = 9.507$ $V = 520.30$ $\beta = 100.70°$	$a = 6.066$ $b = 11.451$ $c = 8.317$ $V = 577.76$

[a] According to ASTM data [9–11].

[b] Present data for the three Mg vanadate phases after calcination at 650°C.

tion temperature increases from 550 to 650°C, especially for MgV_2O_6 phase which has the largest reduction in the surface area.

3.2. SCANNING ELECTRON MICROSCOPY

The SEM examination of the three Mg vanadate phases is shown in fig. 2. The particle sizes and morphologies depended not only on the Mg/V atomic ratio of phases but also on the calcination temperature. α-$Mg_2V_2O_7$ and $Mg_3V_2O_8$ phases after calcination at 550 and 650°C appear to be porous, shapeless particles. The MgV_2O_6 phase after calcination at 550°C consist also of porous, shapeless particles, but calcination at 650°C leads to better defined parallelepipeds with nonuniform sizes (1–6 μm).

3.3. DTA MEASUREMENTS

DTA data for the three Mg vanadate phases after calcination at 550°C are given in table 2. No DTA peak is detected in $Mg_3V_2O_8$ phase during the test. In α-$Mg_2V_2O_7$, an endotherm at 772°C was obtained and can be assigned to an α–β polymorphic transition. In MgV_2O_6, the endotherm at 571°C is assigned to α–β polymorphic transition. At higher temperature around 754°C MgV_2O_6 decomposes into V_2O_5 and β-$Mg_2V_2O_7$. However, the α–β polymorphic transition in MgV_2O_6 phase was found to be reversible after cooling, indicating that this so-called β-form MgV_2O_6 polymorph is not stable and cannot exist at room temperature.

3.4. FT-IR STUDY

Fig. 3 shows the infrared spectra of the three Mg vanadate phases after calcination at 550 and 650°C. Figs. 3b and 3c are ascribed to α-$Mg_2V_2O_7$ and $Mg_3V_2O_8$, respectively. The only change observed in the spectral features with calcination temperature is that the band intensity is higher and reduction is better with higher calcination temperature.

Unlike the other two Mg vanadates, the infrared spectra feature of the MgV_2O_6 phase (see fig. 3a) is dependent on the calcination temperature. A significant change was observed in the position, relative intensity and width of the infrared bands as a function of calcination temperature.

3.5. RAMAN STUDY

The Raman spectra of the three Mg vanadate phases at different calcination temperatures are presented in figs. 4, 5 and 6. Fig. 4 shows the Raman spectra of the $Mg_3V_2O_8$ phase. The spectral features do not change with calcination temperature, indicative of the thermal stability of the $Mg_3V_2O_8$ phase. The better spectral resolution and higher band intensity show that higher calcination temperature results in a better crystallinity of the $Mg_3V_2O_8$ phase.

The Raman spectra of the α-$Mg_2V_2O_7$ phase are shown in fig. 5. After calcination at 550 and 650°C, the phase exhibits the same spectral feature, with bands mainly at 947, 901, 872, 844 and 629 cm^{-1}. When calcined at 700°C, in addition to these bands, new bands appear at 1013, 881, 786, 740, 521 and 118 cm^{-1}. At 750°C, the Raman bands due to α-$Mg_2V_2O_7$ disappear, while the new bands at 1013, 897, 881, 860, 844, 786, 740 and 520 cm^{-1} predominate in the spectra. These bands correspond to β-$Mg_2V_2O_7$, as evidenced by the XRD analysis [13]. The $Mg_2V_2O_7$ calcined at 700°C contains a mixture of both forms, consistent with the proposition that the equilibrium α–β polymorphic transition occurs at this temperature [10].

The Raman spectra of the MgV_2O_6 phase are given in fig. 6. In the calcination temperature region 550–700°C, the phase exhibits bands mainly at 920, 835, 730, 175 and 150 cm^{-1}. A very weak band was observed at $\sim$ 993 cm^{-1} which is due to vanadium oxide. Since the Raman cross section of V_2O_5 oxide was found to be much larger than that of the MgV_2O_6 phase [14], the amount of V_2O_5 oxide impurity should be very small. After calcination at 750°C, the Raman bands at 994, 703, 525 and 405 cm^{-1} due to V_2O_5 oxide and weak bands at 1014 and 881 cm^{-1} due to β-$Mg_2V_2O_7$ were clearly, observed, indicative of the decomposition of a fraction of MgV_2O_6 into V_2O_5 and β-$Mg_2V_2O_7$.

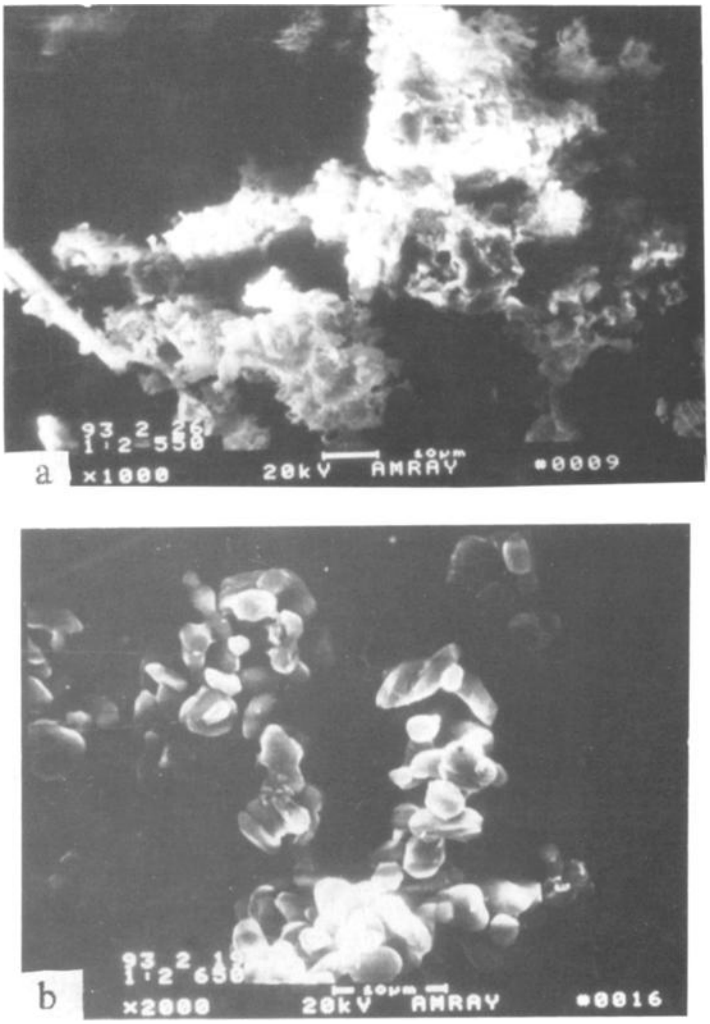

Fig. 2. SEM examination of the Mg vanadate phases at different calcination temperatures. (a) MgV_2O_6 550°C; (b) MgV_2O_6 650°C, (c) α-$Mg_2V_2O_7$ 650°C; (d) $Mg_3V_2O_8$ 650°C.

3.6. THERMOGRAVIMETRICAL STUDY

Fig. 7 illustrates the reduction degree of vanadium ions as a function of time for the MgV_2O_6, α-$Mg_2V_2O_7$ and $Mg_3V_2O_8$ phases calcined at 550°C when reduced at 460°C in hydrogen. A remarkably high reduction speed was obtained with the α-$Mg_2V_2O_7$ phase.

The reduction of the MgV_2O_6 and $Mg_3V_2O_8$ phases exhibits an induction period. Nucleation and growth for the reduction of the MgV_2O_6 phase are slower than for the $Mg_3V_2O_8$ phase.

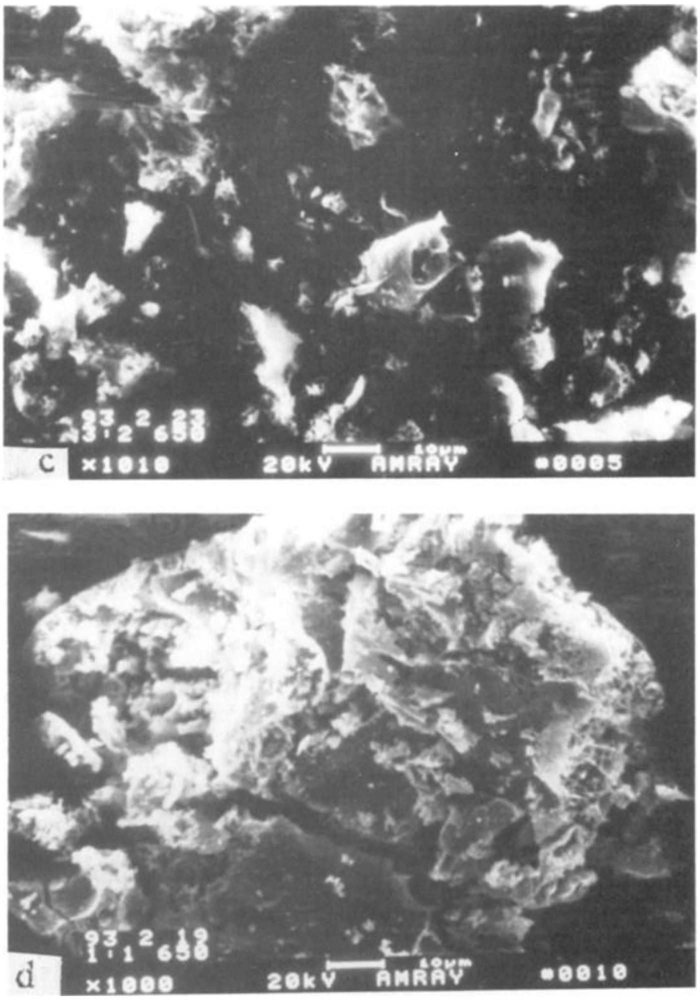

Fig. 2. Continued.

Table 2
DTA data for the three Mg vanadate phases

Compound	Event	Intensity	Peak temp. (°C)	Assignment [a]
$Mg_3V_2O_8$	none			
α-$Mg_2V_2O_7$	endotherm	medium	772	α–β polymorphic transition
MgV_2O_6	endotherm	medium	571	α–β polymorphic transition
	endotherm	very strong	754	peritectic melting to V_2O_5 and β-$Mg_2V_2O_7$

[a] According to Clark [10].

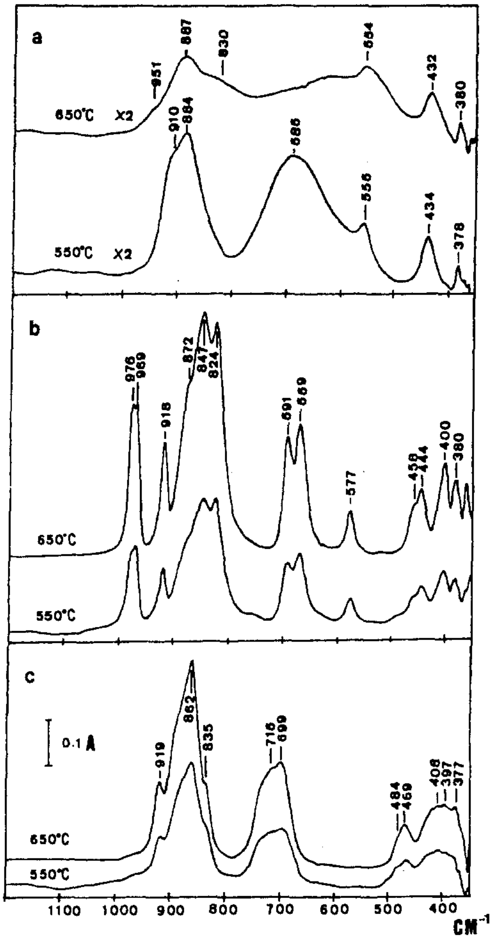

Fig. 3. Infrared spectra of (a) MgV_2O_6; (b) α-$Mg_2V_2O_7$; (c) $Mg_3V_2O_8$.

The reduction curves of the three Mg vanadate phases calcined at 650°C are similar to the curves of the corresponding phases calcined at 550°C, but the rates of reduction are decreased.

The reoxidation experiments were carried out after the vanadate phases have been reduced at certain stages (ca. 10, 20 and 40%). All reduced samples were reoxidized very quickly. No appreciable difference was observed between the different phases.

3.7. CATALYTIC TEST

In the selective oxidation of propane, oxidative dehydrogenation and combustion to carbon oxides are the major reactions over the three Mg vanadate phases. The selectivity as a function of conversion is demonstrated in fig. 8. It can be seen

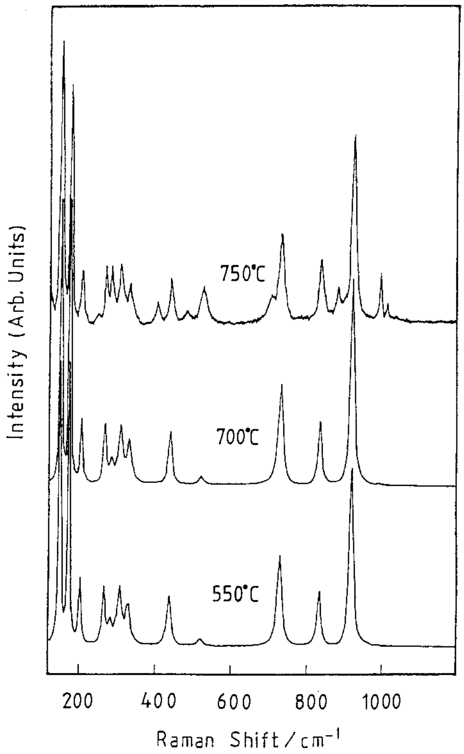

Fig. 4. Raman spectra of MgV_2O_6 phase calcined at different temperatures.

that α-$Mg_2V_2O_7$ has the best selectivity for propene. $Mg_3V_2O_8$ is in the middle. MgV_2O_6 is the worst one, and its selectivity decreases more quickly as the propane conversion increases. Higher calcination temperature of 650°C does not influence the selectivity versus conversion curves of these pure phases.

4. Discussion

The comparison according to literature of IR peak assignments for the three Mg vanadates, which is listed in table 3, shows that except for the MgV_2O_6 phase, there is a good agreement between the different works. The spectrum we obtained after calcination of the MgV_2O_6 at 650°C is closer to the spectrum obtained by Kung and co-workers [4]. Their calcination temperature was also 650°C, but with a longer time (48 h). The calcination temperature used by Volta and co-workers [3] was higher (700°C, 24 h), giving rise to a more distorted infrared spectrum of the MgV_2O_6 phase. The difference in the infrared spectra of the MgV_2O_6 phase is mostly located in the higher wavelength region 600–960 cm^{-1}. This behavior appears to be associated with the very small surface areas (< 1 m^2/g) or great parti-

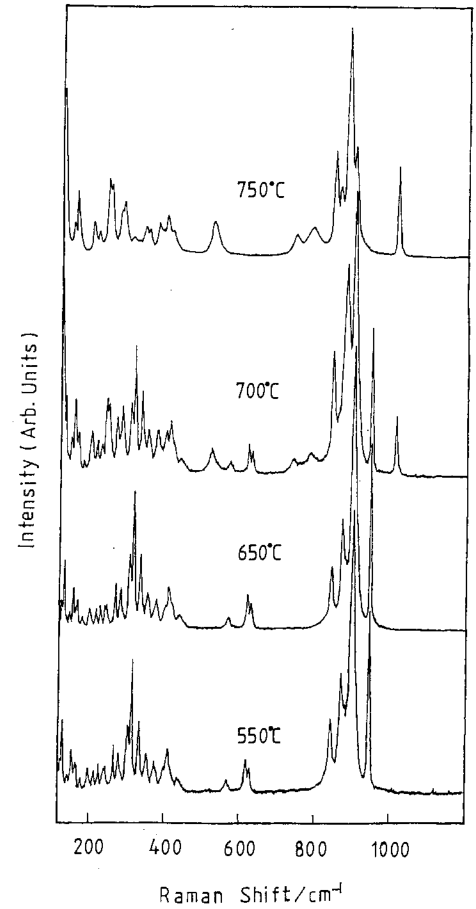

Fig. 5. Raman spectra of α-$Mg_2V_2O_7$ phase calcined at different temperatures.

cles of this phase after high temperature calcination ($\geqslant$650°C) [3,4]. It is known that for greater particles with sizes comparable to the wavelengths of the radiation, nonhomogeneous polarization will cause the infrared spectrum of a powder to vary with the size of the particles [12]. The SEM examination presented above clearly shows that calcination at 650°C results in better defined big particles (~ 1–6 μm), and even higher calcination temperature at 700°C gives rise to a more poorly resolved and less intense spectrum of the MgV_2O_6 phase (not shown here) which is closer to the spectrum obtained by Volta and co-workers [3]. Therefore, the different infrared spectra of the MgV_2O_6 phase obtained by those authors [3,4,6] can be explained by the various preparation conditions which control the particle size and/or morphology of this phase.

The Raman results obtained in the present work are also compared with the previously published data, as presented in table 4. It was thought that some of the previous peak assignments are questionable and may be due to the presence of some

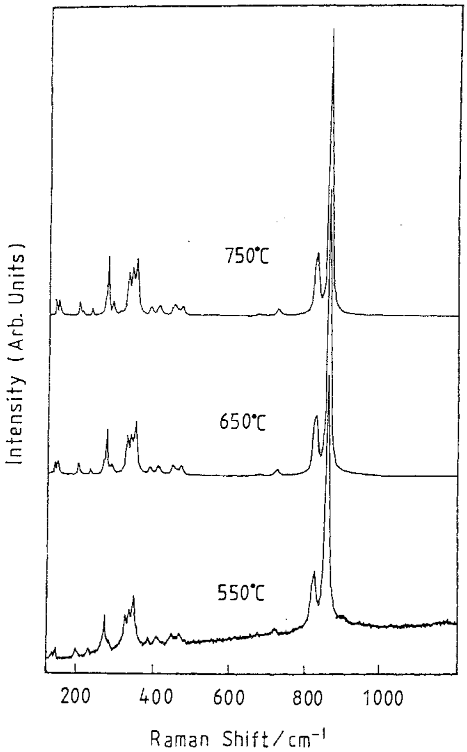

Fig. 6. Raman spectra of $Mg_3V_2O_8$ phase calcined at different temperatures.

impurities. For the α-$Mg_2V_2O_7$ phase, the Raman bands we obtained are very similar to the bands observed by Hardcastle and Wachs [7]. The exception is the band at 726 cm^{-1}. Since the Raman cross section of Mg metavanadate was found to be much larger than that of Mg pyrovanadate phase [14], we are of the opinion that the 726 cm^{-1} band should be attributed to the presence of very small amounts of Mg metavanadate phase. The Raman bands observed at 1008, 897, 881, 846 and 785 cm^{-1} by Hanuza and co-workers [6] for the α-$Mg_2V_2O_7$ phase are certainly ascribed to the β-$Mg_2V_2O_7$ phase.

From the results discussed above, differences in the infrared and Raman data of these phases can be explained by the presence of some phase impurities, and in the case of MgV_2O_6 phase by the difference in sizes and/or morphologies of particles which are controlled by the preparation conditions. It will be shown in the next report [14] that the phase impurities also affect the catalytic behavior of the Mg vanadate phases.

The characterization results presented above confirm that MgV_2O_6, α-$Mg_2V_2O_7$ and $Mg_3V_2O_8$ can be successfully prepared with high phase purity form very homogeneous Mg–V–citrate precursors at a relatively low calcination temperature (550°C).

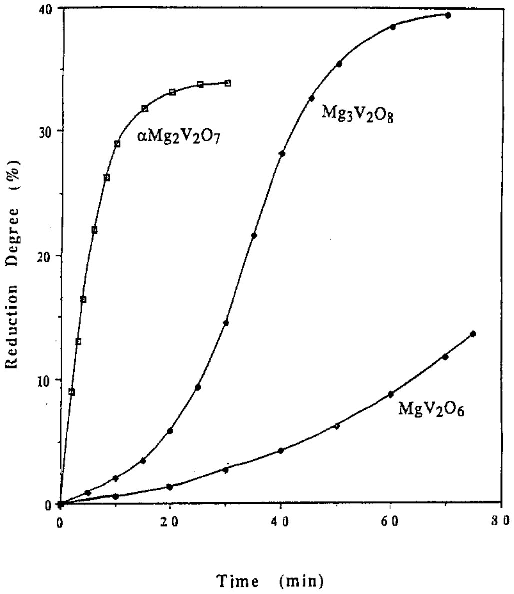

Fig. 7. Thermogravimetrical study of H_2-reduction at 460°C on three Mg vanadate phases calcined at 550°C.

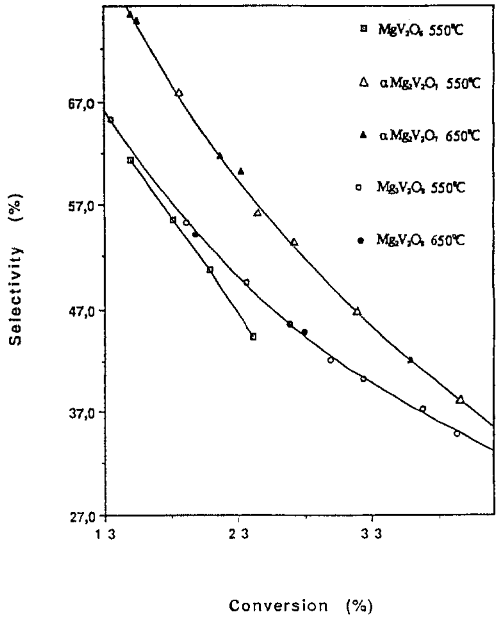

Fig. 8. Effect of propane conversion on propene selectivity. Catalytic conditions: $T = 540°C$; propane/oxygen = 1/2, and total flow rate = 50 ml/min.

Table 3
Comparison of IR peak assignments for three Mg vanadates

MgV_2O_6				α-$Mg_2V_2O_7$			$Mg_3V_2O_8$			Assignment[a]
H[a]	S[b]	Pr[c]		H[a]	S[b]	Pr[c]	H[a]	S[b]	Pr[c]	
		650°C	550°C							
950	960	950		980	977	976				ν(Vv=O) and ν_S(VO4)
					965	969				
			910	926	919	918	915	916	919	
883	888	887	884	873	875	872				ν_{AS}(VO4) and ν_{AS}(VO6)
		830		856	850	847	863	865	862	
				815	821	824	827	833	835	
740	740			715				715	716	ν_{AS}(VOV)
			685		692	691	695	696	699	
					668	669				
					575	577				ν_S(VOV)
530	535	554	556	535				485	484	
							477	470	469	
				472			464			δ_S(VO4) and δ_S(VO6)
					456	458				
				440	440	444				
428	425	432	434							
406				400	395	400		405	408	
				390	380	380			397	
373	375	380	378	381			369	373	377	

[a] According to Hanuza [6].
[b] According to Volta and co-workers [3].
[c] Present results.

In the oxidative dehydrogenation of propane over the three pure vanadates, the α-$Mg_2V_2O_7$ phase presents the highest selectivity to propene, while the selectivity of the $Mg_3V_2O_8$ phase is lower, and that of the MgV_2O_6 phase is the lowest. Thermogravimetrical study of reducibility on the three Mg vanadates indicates that their reducibility follows the order: α-$Mg_2V_2O_7 > Mg_3V_2O_8 > MgV_2O_6$. If the catalytic reaction mechanism is as suggested through the redox cycle between V^{5+} and V^{4+} [1,3], the good redox behavior under reaction conditions might be favorable for the selective oxidation of propane. Based on the high reoxidation rates of the three vanadates, the redox property is also like α-$Mg_2V_2O_7 > Mg_3V_2O_8 > MgV_2O_6$. This order suggests that there might be present a correlation between the catalytic property and the redox property of the pure Mg vanadate phases.

Table 4
Comparison of Raman frequencies of three magnesium vanadate phases

MgV_2O_6		α-$Mg_2V_2O_7$				$Mg_3V_2O_8$	
Pr[a]	H[b]	Pr[a]		H[b]	W[c]	Pr[a]	H[b]
		650°C	750°C				
920 vs	932 vs	947 s	1013 s	1008 s	942		
835 m	846 s	901 vs	897 m	897 w	896	861 vs	868 vs
		872 m	881 vs	881 s	867	826 s	833 s
	797 w		860 m	861 m			828 m
730 s	745 s	844 m	844 s	846 s	838	723 w	
			786 m	785 m	726		
		629 w	740 m		629	671 vw	541 m
520 w	530 s	620 m			617		524 m
	495 w	568 w	521 m	526 m	566		484 m
439 m	450 s	438 w	412 w	410 w	440	470 w	462 m
	383 w	418 sh	397 m			448 w	448 m
		411 m	374 m	382 w	411	409 w	420 m
		401 sh	350 w			387 w	387 w
		377 w			379		
331 m		354 w	338 m	340 m	358	350 m	344 s
309 m	310 m	335 m			334	340 m	
286 w		317 m			316	329 m	
268 m	274 m	306 m		309 m	306	289 w	296 w
205 m		282 w	283 m	284 s	283	275 m	279 m
175 vs		268 w	274 sh		268	269 sh	
150 vs		247 w	249 m	246 s	200	233 w	
		242 w	242 m			207 vw	
		228 w	216 w			200 w	
		217 w	202 m			145 w	
		199 w	158 m			137 w	
		181 vw	149 w				
		167 w	118 vs				
		156 w					
		147 vw					
		132 m					
		127 w					

[a] Present results.
[b] According to Hanuza [6].
[c] According to Hardcastle and Wachs [7].

Acknowledgement

The authors gratefully acknowledge the support of this work by the "Fonds National de la Recherche Scientifique" of Belgium and the Chinese National Science Foundation. This work is conducted in the form of the "Action Cencertée" of the "Communauté Française de Belgique" from which the Unité de Catalyse et Chimie des Matériaux Divisés benefits. We thank Dr. J. Naud for XRD analysis.

References

[1] M.A. Chaar, D. Patel, M.C. Kung and H.H. Kung, J. Catal. 105 (1987) 483.
[2] M.A. Chaar, D. Patel and H.H. Kung, J. Catal. 109 (1988) 463.
[3] D. Siew Hew Sam, V. Soenen and J.C. Volta, J. Catal. 123 (1990) 417.
[4] D. Patel, M.C. Kung and H.H. Kung, in: *Proc. 9th Int. Congr. on Catalysis*, Vol. 4, Calgary 1988, eds. M.J. Phillips and M. Ternan (Chem. Inst. of Canada, Ottawa, 1988) p. 1553.
[5] M.C. Kung and H.H. Kung, J. Catal. 134 (1992) 668.
[6] J. Hanuza, B. Jerowska-Trebiatowska and W. Oganowski, J. Mol. Catal. 29 (1985) 109.
[7] F.D. Hardcastle and I.E. Wachs, J. Phys. Chem. 95 (1991) 5031.
[8] Ph. Courty, H. Ajot, Ch. Marcilly and B. Belmon, Powder Technol. 7 (1973) 21.
[9] A. Nord et al., Chim. Scripta 25 (1985) 212 (ASTM file No. 37-351).
[10] G. Clark and R.J. Morley, J. Solid State Chem. 16 (1976) 1429 (ASTM file No. 31-816).
[11] F. Parker and McCauley, private communication (ASTM file No. 34-13).
[12] M. Ocana, V. Fomes, J.V. Garcia Ramos and C.J. Serna, J. Sol. Stat. Chem. 75 (1988) 364.
[13] R. Gopal and C. Calvo, Acta. Cryst. B 30 (1974) 2491 (ASTM file No. 29-877).
[14] X.T. Gao et al., submitted.